Chinese Science Bulletin

The program structure designing and optimizing tests of GRAPES physics

XU GuoQiang[1†], CHEN DeHui[1,2], XUE JiShan[1], SUN Jian[1], SHEN XueShun[1], SHEN YuanFang[1], HUANG LiPing[1], WU XiangJun[1], ZHANG HongLiang[1] & WANG ShiYu[1]

[1] State Key Laboratory of Severe Weather, Chinese Academy of Meteorological Sciences, Beijing 100081, China;
[2] National Meteorological Centre, Beijing 100081

According to the modularization and standardization of program structure in Global/Regional Assimilation and Prediction System (GRAPES), the plug-compatible and transplantable regional meso-scale and global middle-range physics software package is established. The package's component integrality is comparative with the other advanced models physics. A three-level structure of connecting GRAPES physics and dynamic frame has been constructed. The friendly interface is designed for users to plug in their own physics packages. Phenomenon of grid-point storm rainfall in numerical prediction is analyzed with the numerical tests. The scheme of air vertical velocity calculation is improved. Optimizing tests of physics schemes are performed with the correlative parameters adjusting. The results show that the false grid-point storm rainfall is removed by precipitation scheme improving. Then the score of precipitation forecast is enhanced.

physics, program structure, grid-point storm rainfall, optimizing numerical tests

Representation of physical processes in a numerical weather prediction (NWP) model has significant effects on the model's performance. Therefore, whether it is a global model or a regional model, the NWP model should incorporate physics schemes as perfect and detailed as possible. The physics schemes normally include representations of microphysics, cumulus convection, radiation, land surface processes, turbulence, boundary layer processes. Integration and unification of the physics schemes has become a trend in recent years. Many countries have been trying to develop a unified program package that includes various advanced physics schemes. At the same time, model developing groups are trying to integrate global model and regional model into an integrated model system with the same dynamic framework and multiple optional physics schemes.

The Global/Regional Assimilation and Prediction System (GRAPES) is a new generation NWP system independently developed by Chinese[1−3]. Various state-of-the-art physics schemes are incorporated into the GRAPES. These schemes are evaluated through short- (2−3 days) and middle-range (5−10 days) simulations of precipitating weather events occurred in China and are then optimized appropriately. The GRAPES consists of two sub-systems: the regional meso-scale numerical forecast system and the global middle-range forecast system. For the regional meso-scale numerical forecast system, the key physical processes include cloud microphysics, radiation, surface layer, land surface, planetary boundary layer, turbulence and other physical processes, with a focus on cloud microphysics and planetary boundary layer processes. For the global middle-range forecast system, representations of cloud-radiation feedback, cumulus convection, and atmosphere bound-

Received December 26, 2007; accepted June 4, 2008
doi: 10.1007/s11434-008-0418-y
†Corresponding author (email: xugq@cma.gov.cn)
Supported by National Key and Technology Research and Development Program (Grant Nos. 2006BAC02B03, GYHY200706045 and GYHY200706005), National Natural Science Foundation of China (Grant Nos. 40775063 and 40575050), and National Basic Research Program of China (Grant No. 2004CB418306)

ary layer process are the most important. Currently, a plug-compatible physics software package that incorporates representations (explicit or parameterization) of the physical processes to be used in both the regional meso-scale and the global middle-range forecast sub-systems has been established. By coupling the physics package with the dynamic framework of the GRAPES, the Chinese new generation prototype numerical prediction system for both regional meso-scale and global middle-range forecast is developed. The new system can be applied to different regions of China. To improve the model's prediction abilities for precipitating weather events occurred in China, the physics needs further improvement through optimization of the schemes introduced from other countries. The final goal is for the new system to be used at the operational NWP centers of China.

1 Components of the GRAPES physics schemes

As in other state-of-the-art meso-scale and middle-range forecast models, four categories of physics program modules are implemented in GRAPES: cloud and precipitation process, boundary layer process, land surface process, and radiative transfer process. The physics schemes incorporated in the European Center for Medium range Weather Forecasting (ECMWF) global forecasting model and the United States Weather Research and Forecast (WRF) model have been implemented into the GRAPES. The plug-compatible and transplantable physics software package for both the regional meso-scale and the global middle-range forecasts are established to couple with the dynamic framework of the GRAPES. Numerical experiments have been conducted for precipitating events occurred in China and important parameters/processes are adjusted to optimize the physics schemes.

The GRAPES physics software package mainly includes convective precipitation process[4–8], stratiform cloud and precipitation process[9–14], radiation process[15–21], and land surface and boundary layer process[22–25]. Table 1 provides a comparison of the optional physics schemes between the GRAPES and the United States WRF model (version 1.3). It is shown that some physics schemes in the GRAPES have been improved by the Chinese scientists and are more suitable for the Chinese weather conditions. For example, ice frozen process has been added to the CAMS simple ice scheme[13] so that masses of supercold liquid water and ice crystal are predicted. In CAMS mixed ice scheme[14], the forecasting variables are the contents of cloud water, rain water, ice crystal, snow and graupel, the number concentrations of rain water, ice crystal, snow and graupel, as well as the topologic wide functions of autoconversion efficiency of cloud water, rain water, snow and graupel. This scheme includes more complete cloud microphysical processes at the expense of increased computation costs. In general, the completeness of the GRAPES physics schemes is comparable to other advanced NWP models on the world.

Table 1 Comparison of the optional physics schemes between the GRAPES and WRF model

Physics	Explicit precipitation	Cumulus	Long-wave radiation	Short-wave radiation	Surface layer	Land surface	Boundary layer
GRAPES	(1) Kessler (2) Lin (Purdue) (3) NCEP simple ice (4) NCEP mixed phase (5) Eta old microphysics (6) Eta new microphysics (7) CAMS simple ice (8) CAMS mixed phase (9) ECMWF large-scale precipitation	(1) New Kain-Fritsch (2) Betts-Mille-Janjicr (3) Kain-Fritsch	(1) RRTM (2) GFDL (3) ECMWF	(1) Dudhia simple short wave (2) DFDL (3) GSFC (4) ECMWF	(1) Similarity theory (2) MYJ surface scheme	(1) Thermal diffusion (2) OSU/MM5 LSM (3) NCAR LSM	(1) MRF (2) Mellor-Yamada-Janjic (3) Second-order turbulence closure
WRF	(1) Kessler (2) Lin(Purdue) (3) NCEP simple ice (4) NCEP mixed phase (5) Eta old microphysics (6) Eta new microphysics	(1) New Kain-Fritsch (2) Betts-Mille-Janjicr (3) Kain-Fritsch	(1) RRTM (2) GFDL	(1) Dudhia simple short wave (2) DFDL (3) GSFC	(1) Similarity theory (2) MYJ surface scheme	(1) Thermal diffusion (2) OSU/MM5 LSM	(1) MRF (2) Mellor-Yamada-Janjic

2 Program structure of GRAPES physics

The physics schemes of the GRAPES are programmed in accordance with the modular requirement and in a way similar to what utilized by the WRF model[1)]. The variables of each process program module are registered first. Then the three-level structure of each physics module is designed (Figure 1), as described below.

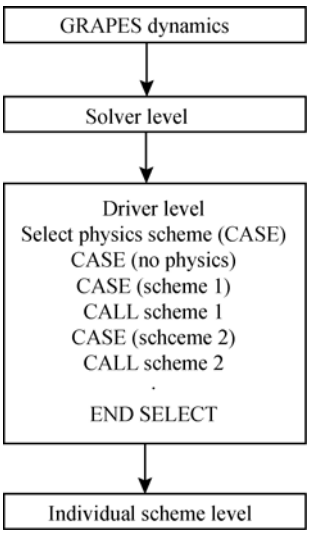

Figure 1 Diagram of the three-level structure of the GRAPES physics program module.

(1) Solver level. The solver level is the interface that connects the dynamics framework with the physics package. The delivery and exchange of variables between the dynamics and the physics schemes is completed at this level.

(2) Driver level. There is a single driver for each physics process that consists of one or multiple schemes. The driver level connects the individual physics scheme with the solver level. The design of the driver level provides a plug-compatible environment for users to plug in their own physics packages.

(3) Individual scheme level. Each physical scheme is a module, consisting of all the subroutines related to the scheme. The individual scheme level is connected to the dynamic framework through the driver level.

The integration of the GRAPES physics module and the GRAPES unified dynamic framework has formed a new generation transplantable NWP system of China that can be used for both regional meso-scale and global middle-rang forecast. The dynamics framework can be either hydrostatic or non-hydrostatic equilibrium. The prediction domain, grid resolutions, physics schemes, output variables and other aspects can also be set by users to satisfy their needs for both research and operations.

3 Optimization of the GRAPES physics schemes

Ensemble numerical experiments were designed to investigate the sensitivity on grid resolutions and physics schemes of the regional meso-scale GRAPES model. Analyses of the results from the experiments demonstrate that the regional GRAPES model is able to reasonably simulate the occurrences and evolution of the high-influential precipitating events occurred in China. Simulations using the regional GRAPES model with high resolutions (15 km in the horizontal) can reproduce the structure and characteristics of typhoon as well as the distributions of meteorological variables as revealed by observations. Based on these, we can say that the GRPARES model has great potential in operational applications. The regional GRAPES system is operationally run at the National Meteorological Center of the Chinese Meteorological Administration and some regional NWP centers of China during 2007.

The numerical experiments also suggest some biases/drawbacks in the prediction. One example is the systematic bias in geopotential height around the Qinghai-Tibet plateau. Another is the false prediction of heavy rainfall, which is not uncommon to NWP model, this phenomenon is usually known as the grid-point storm rainfall in NWP research. The most possible cause for the false prediction of heavy rainfall is probably uncertainties associated with the cloud microphysics scheme.

3.1 Optimization of the precipitation scheme

3.1.1 Problem: false prediction of heavy rainfall by the GRAPES. Numerical experiments suggest that the false prediction of heavy rainfall in the GRAPES is mainly caused by the grid-scale precipitation scheme in the model, which is related to an abnormal increase in the vertical velocity. The overestimate in the magnitude of precipitation is accompanied by overestimated latent heating that warms the atmosphere temperature. Warmer atmosphere favors stronger updraft, and then brings

1) Chen S H, Dudhia J. Annual report: WRF physics. http://www.wrf-model.org, 2000

more condensation. Thus a positive feedback could form. To eliminate the false grid-point storm rainfall phenomenon, the vertical speed calculation was improved and the precipitation scheme was adjusted as described below.

3.1.2 Solution No. 1: inclusion of precipitation drag in the vertical velocity equation. The equation to calculate the change of vertical velocity can be represented as:

$$\frac{\mathrm{d}w}{\mathrm{d}t} \equiv -C_p \overline{\theta} \frac{\partial \Pi'}{\partial z} + g\left(\frac{\theta'}{\overline{\theta}} + 0.608q_v - q_L - q_I\right) + F_w,$$

where $g(0.608q_v - q_L - q_I)$ is the effect of precipitation drag on the change of vertical speed. This term is negative when the sum of liquid water q_L and solid water q_I item is nonzero. That is, the effect of precipitation drag is to decrease the vertical speed and thus reduce the grid-scale precipitation. However, this precipitation drag term was ignored in the previous versions of the GRAPES, which could contribute to the occurrence of false prediction of heavy rainfall by the model.

3.1.3 Solution No. 2: modification of the criteria to trigger grid-scale precipitation. In reality, a large precipitating region is normally in accordance with a large area of updrafts. Yet in numerical prediction, it was found that the false grid-point storm rainfall mainly occurred at a few grid points with abnormally large amount of precipitation and strong updrafts. Inclusion of precipitation drag effect does lighten the false prediction of grid-point storm rainfall, yet does not eliminate it. To further reduce the false prediction of grid-point storm rainstorm by the GRAPES, we modified the criteria to trigger the grid-scale precipitation. One of the original criteria is, as long as one grid point has updraft, there is a possibility for precipitation to occur at this grid point. This criterion is refined to——there is a possibility for precipitation to occur only if this grid point and three grid points surrounding it have updrafts.

The following Section describes a case study to show that the problem of grid-point storm rainfall is largely solved using above methods.

3.2 Numerical experiments to eliminate false prediction of grid-point rainstorm

3.2.1 Design of numerical experiments. The case of July 8, 2003 is simulated with the GRAPES model. Three experiments are conducted. The same configuration is used for these experiments. The grid spacing is 0.5625° (approximately 60 km) in the horizontal. There are 31 layers with varying grid spacing in the vertical. The model integration starts at 0000 UTC July 8, 2003. The physical period of the integration is 36 hours. The time step is 180s. The major physics schemes utilized are: the ECMWF large scale precipitation scheme, the RRTM long wave and Dudhia short wave radiation scheme, the M-O approximate ground surface layer scheme, the thermal diffusion land surface process scheme, the MRF boundary layer scheme, and the Kain-Fritsch convection parameterization scheme.

The experiments differ in the calculation of vertical velocity and/or the trigger of grid-scale precipitation. In one experiment (denoted as EXP1), the original physics schemes are used. In another experiment (denoted as EXP2), the effect of precipitation drag on vertical speed is included. The third experiment (denoted as EXP3) utilizes the refined criteria to trigger grid-scale precipitation as well as includes the effect of precipitation drag on vertical speed.

3.2.2 Results from the numerical experiments. Figure 2(a), (b), (c), (d) depicts the longitude-latitude distributions of surface precipitation during the 36-h period from 00 UTC July 8 to 12 UTC July 9 from the observations as well as the 36-hour rainfall forecast from the three experiments (EXP1, EXP2 and EXP3), including both the grid-scale precipitation and the parameterized subgrid- scale precipitation. The observed precipitation has mainly four large precipitation areas (see Figure 2(a)). The largest rainfall area is in the Jianghuai river basin, distributed from NE towards SW with a maximum of about 300 mm located near (29°N, 111°E). The other three precipitating area are located in the northeast China, the eastern part of Qinghai-Tibet Plateau, and from the southern part of Guangxi to Hainan Province, respectively, with maxima being less than 100 mm. How are the precipitation forecasts from the three numerical experiments compared to the observations? As we can see from Figure 2(b), (c) and (d), distributions of the predicted rainfall bands are similar among the three experiments. The shape and direction of the predicted Jianghuai rainfall band agree with the observation. However, the predicted rainfall area in the eastern China is located slightly too south compared to the observed. The three experiments also predict precipitation at the other three regions where precipitation was observed. The shapes of the rainfall bands predicted by EXP3 are relatively closer to the observation. The intensities of pre-

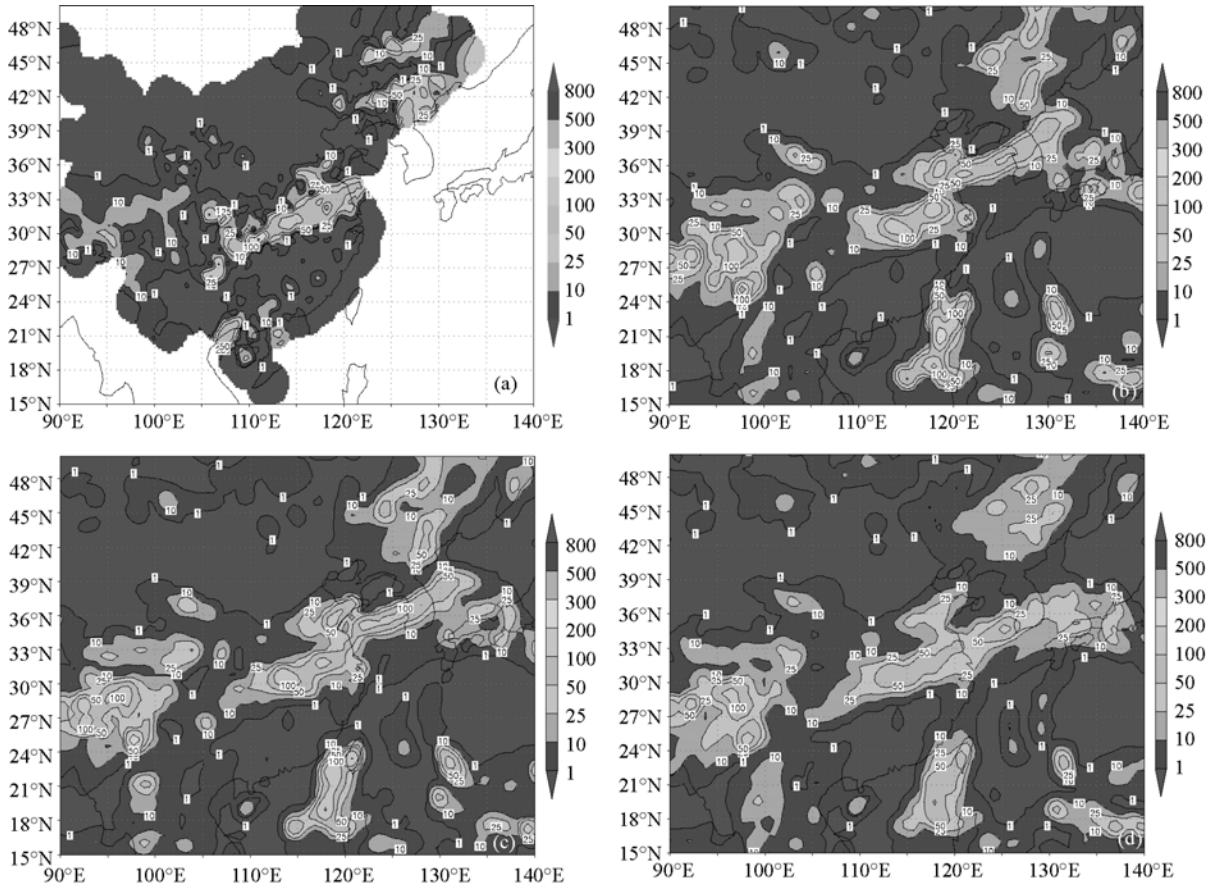

Figure 2 Accumulated surface precipitation of the observed and predicted during the period of 00Z of July 8 to 12Z of July 9. Unit: mm. (a) Observation; (b) EXP1; (c) EXP2; (d) EXP3.

cipitation from the three numerical experiments differ from the observed. The precipitation center near (29°N, 111°E) around the Jianghuai river basin was not predicted by all experiments. The precipitation maxima are too small (< 200 mm from EXP1 and EXP2 and < 100 mm from EXP3) and located too east compared to the observations. However, the 50 mm contour of EXP3 was closer to the observation. The precipitation amounts from the three experiments at northeastern China and the southern part of Guangxi to Hainan Province in China generally agree with the observation except for that EXP3 precipitation is slightly smaller than the observation. For the eastern part of Qinghai-Tibet Plateau, precipitation intensity was too large in EXP1 and EXP2 with maxima of about 1000 mm around the grid point (25°N, 97.5°E). This false grid-scale storm rainfall phenomenon did not occur in EXP3. This false precipitation was mainly produced by the grid-scale precipitation scheme rather than the parameterized subgrid-scale precipitation.

Figure 3 shows the time series of the grid-scale precipitation on the grid point (25°N, 97.5°E) from the experiments. Precipitations from EXP1 (black line in Figure 3) and EXP2 (green line in Figure 3) increase with time reaching maxima of 1300 mm and 850 mm at 12 h and 18 h, respectively. This suggests that grid-point rainstorm occurs when the large-scale precipitation scheme is applied with the original trigger criteria even when the effect of precipitation drag on vertical velocity change is included. When the more constrained criteria for grid-scale precipitation to occur is combined with inclusion of the precipitation drag effect on vertical velocity (EXP3), the accumulated precipitation (yellow line in Figure 3) reaches a maximum of about 120 mm at 8 h, which is comparable to the observed typical values.

To further investigate the possible causes for the occurrences of false grid-point rainstorm, time-pressure cross sections of temperature, specific humidity and vertical speed on the grid point (25°N, 97.5°E) from the three experiments are compared. These results are quite similar between EXP1 and EXP2. Therefore, the results from EXP2 and EXP3 are given in Figure 4(a), (b). As

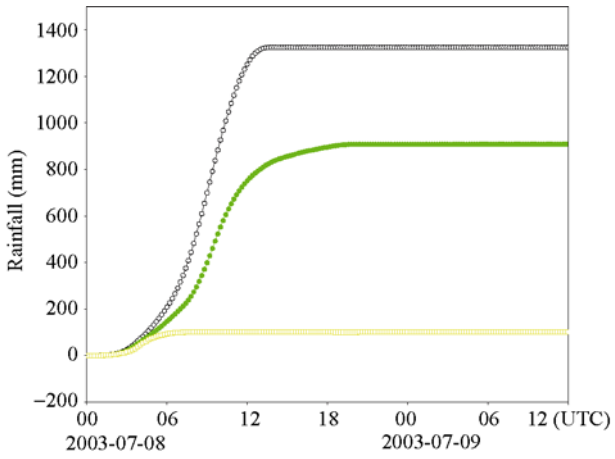

Figure 3 Time series of the grid-scale surface precipitation at the grid point (25°N, 97.5°E) from EXP1 (black line), EXP2 (green line) and EXP3 (yellow line). Unit: mm.

we can see in Figure 4(a), the vertical speed reaches a magnitude of a few meters per second (m s^{-1}) at the middle and upper troposphere, caused by extremely large latent heating which enhanced the updraft and intensified condensation in EXP2. This positive feedback continues until the humidity drops to the degree that it could not maintain the production of precipitation. This might be the mechanism for the occurrence of false grid-point rainstorm. What's accompanying is the occurrences of an abnormally strong warm and moisture center (Figure 4(a)) to maintain the abnormal grid-point rainstorm. The difference between EXP2 and EXP1 (not shown) is mainly that the maximum of vertical speed at the middle-and-upper troposphere was slightly smaller, and the warm center and moisture center were a little weaker, suggesting that the false grid-point rainstorm phenomenon was alleviated in EXP2. In EXP3 (Figure 4(b)), the maximal vertical speed was less than 1 m s^{-1}. There were a weak warm and moisture center extending from the ground surface to 300 hPa. The temperature contours becomes flat at and above 300 hPa, indicating little change with time. Based on these, we concluded that there was no false abnormal marshal of meteorological elements in EXP3.

In the prediction of the vertical speed, the effect of precipitation drag should be included. The criteria for grid-scale precipitation to occur are more constrained in EXP3. These modifications result in reduced maxima in precipitation amount, with little change in the location and domain of surface rainfall. While eliminated the false grid-point rainstorm and improved the accuracy of surface precipitation forecast, these modifications to the grid-scale precipitation scheme and the vertical velocity prediction also increased numerical calculation stability of the model. In general, prediction of the surface precipitation is more satisfactory with these modifications. We conclude that the optimization of the grid-scale precipitation scheme and the vertical velocity calculation can at least partially eliminate the false grid-point rainstorm and improve precipitation forecasting accuracy. However, there are many other possible reasons for the occurrences of false grid-point rainstorm such as the topography treatment. More studies are needed to address this issue more completely.

Other modifications to the GRAPES physics schemes that we have made include (1) improving the radiation scheme through including the effect of geographical slope on radiation, (2) improving the land surface

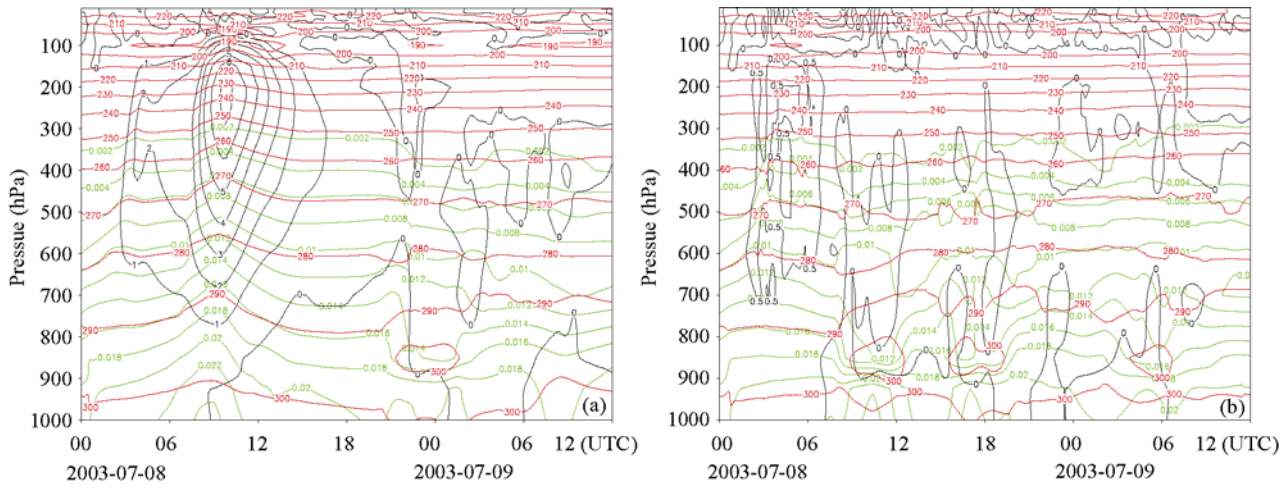

Figure 4 Time-pressure cross sections of temperature (red lines), specific humidity (green lines), and vertical speed (black lines) on the grid point (25°N, 97.5°E) from EXP2 (a) and EXP3 (b). The units are K, kg kg^{-1}, and m s^{-1}, respectively.

scheme by using the most recent datasets to describe surface properties, and (3) introduction of the geographical gravity wave drag scheme in the ECMWF model. These topics are out of the scope of the present paper and will be described in another paper.

4 Conclusions

(1) The new generation GRAPES is developed, which consists of a dynamics framework and a plug-compatible and transplantable physics software package for both regional meso-scale and global middle-range forecasts. On the basis of broad exploration and priority selection of advanced model physics, the software package includes representations of cloud and precipitation process, boundary layer process, land surface process, radiation energy transporting process and other physics processes. The software package is modularized and standardized, and the physics schemes are optimized for better performance in predicting weather events occurred in China. This solved the key issue of physics program package that is needed for numerical weather prediction of China.

(2) A three-level program interface is designed for the new generation GRAPES. The interface connects model physics with dynamics by providing a user-friendly platform for the plug-in use of physics software package. The GRAPES physics modules are integrated with the unified dynamic framework, which can be used as either a regional meso-scale or a global middle-range numerical weather prediction system. The dynamics framework can be either hydrostatic or non-hydrostatic equilibrium. The forecasting domain, grid resolutions, physics schemes, and output variables are set by the users.

(3) Aiming at eliminating the false prediction of grid-point rainstorm, effect of precipitation drag on vertical speed calculation is included and the criteria to trigger the grid-scale precipitation are refined. Numerical experiments show that these modifications have at least partially removed the false grid-point rainstorm phenomenon and improved the accuracy of surface precipitation forecast.

1 Chen D H, Xue J S, Yang X S, et al. New generation of multi-scale NWP system (GRAPES): general scientific design. Chin Sci Bull, 2008, 53(22): 3433－3445
2 Xue J S, Zhuang S Y, Zhu G F, et al. Scientific design and preliminary results of three-dimensional variational data assimilation system of GRAPES. Chin Sci Bull, 2008, 53(22): 3446－3457
3 Zhang R H, Shen X S. On the development of the GRAPES——A new generation of the national operational NWP system in China. Chin Sci Bull, 2008, 53(22): 3429－3432
4 Betts A K. A new convective adjustment scheme. Part I: Observational and theoretical basis. Quart J Roy Meteor Soc, 1986, 112: 677－691
5 Betts A K, Miller M J. A new convective adjustment scheme. Part II: Single column tests using GATE wave, BOMEX, and arctic air-mass data sets. Quart J Roy Meteor Soc, 1986, 112: 693－709
6 Kain J S, Fritsch J M. A one-dimensional entraining/detraining plume model and its application in convective parameterization. J Atmos Sci, 1990, 47: 2784－2802
7 Kain J S, Fritsch J M. Convective parameterization for mesoscale models: The Kain-Fritcsh scheme. Cumulus parameterization. Meteor Monogr, 1993, 46: 165－170
8 Fritsch J M, Chappell C F. Numerical prediction of convectively driven mesoscale pressure system. Part I: Convective parameterization. J Atmos Sci, 1980, 37: 1722－1733
9 Kessler E. On the distribution and continuity of water substance in atmospheric circulation. Meteor Monogr, 1969, 10(32): 1－84
10 Lin Y L, Farley R D, Orville H D. Bulk parameterization of the snow field in a cloud model. J Clim Appl Meteor, 1983, 22: 1065－1092
11 Chen S H, Sun W Y. A one-dimensional time dependent cloud model. J Meteor Soc Japan, 2002, 80: 99－118
12 Hong S Y, Juang H M H, Zhao Q. Implementation of prognostic cloud scheme for a regional spectral model. Mon Weather Rev, 1998, 126: 2621－2639
13 Hu Z J, Lou X F, Bao S W. A simplified explicit scheme of phase mixed cloud and precipitation (in Chinese). Quart J Appl Meteor, 1998, 9(3): 257－264
14 Liu Q J, Hu Z J, Zhou X J. Explicit cloud schemes of HLAFS and simulation of heavy rainfall and clouds, Part I: Explicit cloud schemes (in Chinese). Quart J Appl Meteor, 2003, 14(S1): 60－67
15 Dudhia J. Numerical study of convection observed during the winter monsoon experiment using a mesoscale two-dimensional model. J Atmos Sci, 1989, 46: 3077－3107
16 Fu Q S, Liou K N. Parameterization of the radiative properties of cirrus clouds. J Atmos Sci, 1993, 50: 2008－2025
17 Mlawe E J, Taubman P D, Brown M J, et al. Radiative transfer for inhomogeneous atmosphere: RRTM, a validated correlated-k model for the long-wave. J Geophys Res, 1997, 102(D14): 16663－16682
18 Schwarzkopf M D, Fels S B. The simplified exchange method revisited: An accurate, rapid method for computation of infrared cooling rates and fluxes. J Geophys Res, 1991, 96: 9075－9096
19 Lacis A A, Hansen J E. A parameterization for the absorption of solar radiation in the earth's atmosphere. J Atmos Sci, 1974, 31: 118－133
20 Morcrette J J. Impact of changes to to radiation transfer parameterization plus cloud opitical properties in the ECMWF model. Mon Weather Rev, 1990, 118: 847－873
21 Morcrette J J. Radiation and cloud radiative prpperties in the ECMWF forecasting system. J Geophys Res, 1991, 96: 9121－9132
22 Hong S Y, Pan H L. Nonlocal boundary layer vertical diffusion in a medium-range forecast model. Mon Weather Rev, 1996, 124: 2322－2339
23 Janjic Z I. The step-mountain coordinate: physical package. Mon Weather Rev, 1990, 118: 1429－1443
24 Beljaars A C M. The parameterization of surface fluxes in large-scale models under free convection. Quart J Roy Meteor Soc, 1994, 121: 255－270
25 Janjic Z I. The Mellor-Yamada level 2.5 scheme in the NCEP Eta model. Eleventh Conference on Numerical Weather Prediction, Norfolk, VA, 19－23, August 1996, Am Meteorl Soc, Boston, MA, 333－334